Relative Downlink Channel Calibration in OFDM Systems with CORDIC QR Decomposition

Frank Ludwig*, Mark Petermann**, Dirk Wübben**, Karl-Dirk Kammeyer**, Steffen Paul*
*Institute of Electrodynamics and Microelectronics
Email: {ludwig, steffen.paul}@me.uni-bremen.de
**Department of Communications Engineering
Email: {petermann, wuebben, kammeyer}@ant.uni-bremen.de
University of Bremen, 28359 Bremen, Germany

***Abstract*— Mismatched front-ends reduce the performance of precoding in multi-antenna OFDM systems, which results in a poor bit error rate. With a relative downlink channel calibration the transmission quality will be enhanced. An excellent calibration technique is based on a total least squares optimization problem. For the hardware implementation an efficient fixed-point computation will be presented, which provides a brilliant calibration performance. This approach has low complexity and can efficiently be implemented in hardware by using the CORDIC algorithm.**

I. Introduction

Orthogonal frequency division multiplexing (OFDM) is a very important technique for wireless communication. Especially multi-antenna systems are in researchers' focus, and precoding at the base station (BS) is a well-known technique to improve the transmission performance, e.g., the bit error rate (BER). But for precoding the downlink channel (DL) must be known at the BS. In TDD systems usually the reciprocity of the uplink (UL) and the downlink channel is assumed, then the DL channel is equal to the transposed UL channel which can be estimated at the BS. Another way to get the DL channel at the BS is to feedback the estimated DL channel from the mobile stations (MS) to the BS. Both approaches have disadvantages. Due to mismatched front-end implementations the reciprocity is commonly not given [1]. Also both channels are estimated and usually have an estimation error. These errors lead to a worse performance while using precoding. Another problem is the reduced effective transmitted data in the UL by a feedback of the channel state information (CSI). With a relative calibration of the DL, as in [2], [3], precoding will be usable for systems with non ideal front-ends. The advantage of the relative calibration is that errors in reciprocity and channel estimation will not cause a worse BER. Furthermore, the transmitted data for the DL feedback to the BS can significantly be reduced, because a permanent CSI feedback of the DL is not needed.

The work presented in this article is funded by the German Research Foundation (DFG) under grant PA 438/3-2 and KA 841/21-2.

In this paper the calibration is realized by solving a total least squares (TLS) problem. In general the TLS utilizes the rightmost singular vector, which requires calculation of a singular value decomposition (SVD). To reduce the complexity of the calculation of the SVD, several methods are known [4], as an alternative a partial SVD can be used for the TLS [5]. As only the rightmost singular vector is needed for the TLS solution, a two-sided orthogonal decomposition instead SVD is possible [6]. These decomposition are called URV or ULV decomposition (URVD or ULVD), which generates unitary matrices $\mathbf{U}$, $\mathbf{V}$ and upper or lower triangular matrices $\mathbf{R}$ or $\mathbf{L}$. The matrix $\mathbf{V}$ of ULVD is an approximation of the right singular vector and is used for the calibration in this paper, which nearly reaches the same transmission quality as a calibration with SVD. This paper shows how the calculation of $\mathbf{V}$ can efficiently be implemented in hardware by two QR-decompositions (QRD), which only uses multiplications and additions without any division or square roots.

The remainder of this paper is organized as follows. In Section II the system model is presented. The relative DL channel calibration is described in Section III, where the calibration with use of a TLS-solution is presented and the way how it can be solved by two QR-decompositions. Section IV considers hardware implementation issues of the QRD. Performance evaluation results are shown in Section V. Finally, in Section VI a conclusion and an outlook are given.

II. System Model

A multi-user (MU) MISO-OFDM system with N_C subcarriers is applied. It consists of one BS with

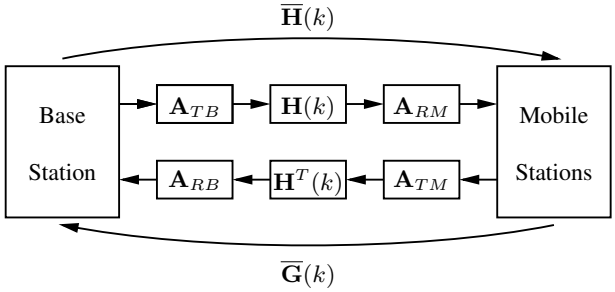

Fig. 1. Simplified channel model with gain mismatch matrices per subcarrier k

N_B antennas and $N_M \leq N_B$ decentralized single-antenna MS. The BS executes a linear precoding. Then, for ideal front-ends the receive signal $\mathbf{y}(k)$ at the MSs per subcarrier k is given by:

$$\mathbf{y}(k) = \beta(k)\mathbf{H}(k)\mathbf{F}(k)\mathbf{s}(k) + \mathbf{n}(k), \qquad (1)$$

where $\mathbf{H}(k)$ denotes the DL channel, $\mathbf{F}(k)$ the precoding matrix, $\mathbf{s}(k)$ the transmitted signal and $\mathbf{n}(k)$ an additive white Gaussian noise vector. The scalar $\beta(k)$ is chosen such that the total sum power constraint per subcarrier is fulfilled [2]. Generally, the quality of the precoding is given by the knowledge of the transmission channel $\mathbf{H}$. Due to mismatched front-ends $\mathbf{H}$ is not perfectly known. In Fig. 1 the channel model with non-ideal front-ends is shown, where the physical DL and UL channels between the antennas is given by $\mathbf{H}$ and $\mathbf{H}^T$, because reciprocity is valid between the antennas. By mismatched real-world front-ends both transmission channels change independently, and the reciprocity assumption is not valid for "digital" channel. In Fig. 1 this is modeled by diagonal gain mismatch matrices $\mathbf{A}_{[R/T][B/M]}$ caused by the receive or transmit components of BS and MS front-ends. The error values in $\mathbf{A}_{[R/T][B/M]}$ are statistically independent zero mean complex Gaussian random variables with variance σ_δ^2 [7]. It can be assumed that these values do not change fast in time and that they are equal for each antenna on all subcarriers k. Considering these front-end mismatches, the effective UL channel is defined by

$$\overline{\mathbf{G}}(k) = \mathbf{A}_{RB}\mathbf{H}^T(k)\mathbf{A}_{TM}, \qquad (2)$$

and the effective DL matrix can be written as

$$\overline{\mathbf{H}}(k) = \mathbf{A}_{RM}\mathbf{H}(k)\mathbf{A}_{TB}\ . \qquad (3)$$

Another error is caused by channel estimation (CE) in the BS and MSs. Based on the MMSE channel predictor model, the estimated DL and UL channels can be written as [7]

$$\tilde{\mathbf{H}}(k) = \sqrt{1-\sigma_e^2}\ \overline{\mathbf{H}}(k) + \sqrt{\sigma_e^2(1-\sigma_e^2)}\ \mathbf{\Psi}_M(k) \qquad (4)$$

and

$$\tilde{\mathbf{G}}(k) = \sqrt{1-\sigma_e^2}\ \overline{\mathbf{G}}(k) + \sqrt{\sigma_e^2(1-\sigma_e^2)}\ \mathbf{\Psi}_B(k)\ , \qquad (5)$$

where $\mathbf{\Psi}_B$ and $\mathbf{\Psi}_M$ are independent Gaussian error matrices with entry variance one and estimation error variance σ_e^2. Due to these errors, precoding on basis of $\tilde{\mathbf{G}}^T$ or $\tilde{\mathbf{H}}$ will deteriorate the transmission performance as true channel is $\overline{\mathbf{H}}$. Now, the aim of the calibration is to provide an approximation of $\overline{\mathbf{H}}$ out of mismatch and CE errors including UL $\tilde{\mathbf{G}}(k)$.

III. Relative DL Channel Calibration

A. Calibration principle

The basic concept of relative DL channel calibration was presented in [3]. The purpose of the calibration is to approximate the DL transmission channel $\overline{\mathbf{H}}$ for precoding in the BS on basis of the estimated UL channel $\tilde{\mathbf{G}}$. By the CE error is ignored, the physical channel $\mathbf{H}(k)$ can be calculated by (2)

$$\mathbf{H}(k) = \mathbf{A}_{TM}^{-1}\overline{\mathbf{G}}^T(k)\mathbf{A}_{RB}^{-1}\ . \qquad (6)$$

Using this result in (3) the relation of both effective channel matrices is

$$\overline{\mathbf{H}}(k) = \underbrace{\mathbf{A}_{RM}\mathbf{A}_{TM}^{-1}}_{\mathbf{C}_M}\overline{\mathbf{G}}^T(k)\underbrace{\mathbf{A}_{RB}^{-1}\mathbf{A}_{TB}}_{\mathbf{C}_B}. \qquad (7)$$

Because $\mathbf{A}_{[R/T][B/M]}$ are diagonal matrices, the two calibration vectors $\mathbf{c}_M \triangleq \text{diag}^{-1}\{\mathbf{C}_M^{-1}\}$ and $\mathbf{c}_B \triangleq \text{diag}^{-1}\{\mathbf{C}_B^{-1}\}$ can be defined[1]. The challenge of calibration is to obtain these vectors $\mathbf{c}_B$ and $\mathbf{c}_M$ so that the transmission channel $\overline{\mathbf{H}}(k)$ can be approximated to

$$\overline{\mathbf{H}}(k) \approx \underline{\mathbf{G}}(k) = \text{diag}\{\mathbf{c}_M^{-1}\}\overline{\mathbf{G}}^T(k)\,\text{diag}\{\mathbf{c}_B^{-1}\} \qquad (8)$$

with the estimated UL. Consequently, the calibrated UL channel is labeled as $\underline{\mathbf{G}}(k)$ for differentiation.

To obtain the two calibration vectors, estimated matrices $\tilde{\mathbf{G}}(k)$ and $\tilde{\mathbf{H}}(k)$ have to be applied in the calibration phase, at least for one subcarrier. Previous works have shown that the more subcarriers are used, the better results achieved by calibration [7]. For this reason it is assumed, that $\tilde{\mathbf{H}}(k)$ is known for K_c subcarriers at BS by feedback. After calibration phase the calibration vectors $\mathbf{c}_M$ and $\mathbf{c}_B$ will be used for calibration. Then, only the actual $\tilde{\mathbf{G}}(k)$, $\mathbf{c}_M$ and $\mathbf{c}_B$ will be used in the BS to calibrate the UL and to calculate $\underline{\mathbf{G}}(k)$ described in (8). $\tilde{\mathbf{H}}(k)$ does not have to be estimated and transmitted to the BS again if the reciprocity error variance σ_δ^2 does not change too much.

[1] $\text{diag}^{-1}\{\cdot\}$ transforms a diagonal matrix into a vector, whereas $\text{diag}\{\cdot\}$ transforms a vector in a diagonal matrix

B. Calibration with TLS

Following [2] and [3], the matrix

$$\mathbf{E}_k = \begin{bmatrix} \mathrm{diag}\{\tilde{\mathbf{h}}^{(1)}(k)\} & -\tilde{\mathbf{g}}^{(1)T}(k) & & \mathbf{0} \\ \vdots & & \ddots & \\ \mathrm{diag}\{\tilde{\mathbf{h}}^{(N_M)}(k)\} & \mathbf{0} & & -\tilde{\mathbf{g}}^{(N_M)T}(k) \end{bmatrix}. \tag{9}$$

can defined for each used subcarrier out of the rows of $\tilde{\mathbf{H}}(k)$ and $\tilde{\mathbf{G}}(k)$[2]. Because K_c subcarriers are used for calibration

$$\mathbf{E} = [\mathbf{E}_1^T, \ldots, \mathbf{E}_{K_c}^T]^T \tag{10}$$

can be composed. With the $K_c N_T N_B \times N_T + N_B$ matrix $\mathbf{E}$ the equation (7) can be reformulated with $\mathbf{c} = [\mathbf{c}_B^T \mathbf{c}_M^T]^T$ to

$$\mathbf{E}\mathbf{c} = \mathbf{0}\ . \tag{11}$$

To calibrate the UL channel the overdetermined system of equations $\mathbf{E}\mathbf{c} = \mathbf{0}$ must be solved. A solution can be found by solving the TLS optimization problem [2]

$$\underset{\Delta\mathbf{E}}{\text{minimize}} \quad \|\Delta\mathbf{E}\|_F \tag{12a}$$

$$\text{such that} \quad (\mathbf{E} + \Delta\mathbf{E})\mathbf{c} \approx \mathbf{0}. \tag{12b}$$

A perturbation matrix $\Delta\mathbf{E}$ must be found with minumum Frobenius norm that lowers the rank of $\mathbf{E}$, where $\Delta\mathbf{E}$ denotes the correction term of the TLS problem. The solution can be calculated by SVD of $\mathbf{E}$ with sorted singular values

$$\mathbf{E} = \mathbf{U}\mathbf{\Sigma}\mathbf{V}^H \tag{13}$$

where $\mathbf{U}$ and $\mathbf{V}$ are unitary matrices and $[\,\cdot\,]^H$ denotes the conjugate transpose. Matrix $\mathbf{V} = [\mathbf{v}_1, \ldots, \mathbf{v}_{N_B+N_M}]$ comprises the right singular vectors $\mathbf{v}_i$. The solution to (12b) is given by the right most singular vector $\mathbf{v}_{N_B+N_M}$, which corresponds to the smallest singular value in $\mathbf{\Sigma}$. The calibration vectors $\mathbf{c}_M$ and $\mathbf{c}_B$ in (7) are calculated by dividing $\mathbf{v}_{N_B+N_M}$ with its last entry

$$\mathbf{c} = -\frac{1}{v_{N_B+N_M, N_B+N_M}} \mathbf{v}_{N_B+N_M}\ . \tag{14}$$

C. TLS with ULVD

Different reduced complexity approaches for calculating the solution vector are known [5], [4], [6]. As described before, the TLS solution comprises of the right most singular vector, the left singular matrix $\mathbf{U}$ and the singular values in $\mathbf{\Sigma}$ are not needed. A good approximation of $\mathbf{V}$ provides the two-sided orthogonal decomposition ULVD. For this decomposition only two QRDs are required, which can efficiently be implemented in hardware. $\mathbf{E}$ must be decomposed such that

$$\mathbf{E} = \mathbf{U}'\mathbf{L}\mathbf{V}'^H \tag{15}$$

where $\mathbf{U}'$, $\mathbf{V}'$ are approximations of $\mathbf{U}$, $\mathbf{V}$ in (13) and $\mathbf{L}$ is a lower triangular matrix. This ULVD will be achieved by

$$\mathbf{E} = \mathbf{Q}\mathbf{R} = \mathbf{Q}\tilde{\mathbf{R}}^H\tilde{\mathbf{Q}}^H \tag{16}$$

$$\text{with} \quad \mathbf{R}^H = \tilde{\mathbf{Q}}\tilde{\mathbf{R}} \tag{17}$$

where $\mathbf{Q} \triangleq \mathbf{U}'$, $\tilde{\mathbf{Q}} \triangleq \mathbf{V}'$ and $\tilde{\mathbf{R}}^H \triangleq \mathbf{L}$. Then the right most column of $\tilde{\mathbf{Q}}$ contains the solution vector $\mathbf{c}$.

IV. QRD Hardware Implementation issues

A. QR Decomposition

In order to reduce the amount of hardware for calibration and to achieve a good quality of transmission, some considerations on the arithmetic precision, calculation complexity and computing time must be made. Because the DL channel estimation is known at the BS during the calibration phase, the precoding can be performed in this term on basis of the estimated DL. So there is a latency until the calibration vectors are needed. Also the assumption that the reciprocity error does not change fast, makes the calibration time less critical. Thus, slower algorithms, which use fewer hardware, can be chosen or the saved hardware can be spent to reach a higher precision. The precision is critical for achieving a good performance.

To compute the QRD especially three methods are established: the Gram-Schmidt process, Householder transformations and Givens rotations. In this paper, Givens rotations are used because costly divisions and square root operations should be avoided. Another advantage of the Givens rotation approach is, that the QRD can adaptively be implemented in hardware. If this is considered in the design, the QRD can be used for undefined numbers of K_c. There are only limitations in matrix-memory. In this way, an adaptive calibration is possible. Because the number of columns of $\mathbf{E}$ are independent of K_c, the Givens rotations can be parallelized for a fixed number of columns. If K_c is incremented only the computing time is rising slightly.

Because $\mathbf{E}$ is overdetermined the first QRD in (16) can be rewritten into

$$\mathbf{E} = \mathbf{Q} \cdot \begin{pmatrix} \mathbf{R}' \\ \mathbf{0} \end{pmatrix}. \tag{18}$$

[2] $\tilde{\mathbf{h}}^{(i)}(k)$ describes the i-th row of matrix $\tilde{\mathbf{H}}(k)$.

Then the second QRD in (17) is performed on $\mathbf{R}'^H$. Note that the dimension of $\mathbf{R}'$ only depends on the number of BS antennas N_B and the number of users N_M. Also the orthogonal matrix $\mathbf{Q}$ in (16) or (18) is not needed and the computional complexity is significantly reduced, if it is not calculated.

B. CORDIC Algorithm

The CORDIC algorithm is a well-known iterative method to calculate trigonometric and algebraic functions like sine, cosine, square root or division [8], [9]. The principle of CORDIC is to do serial micro rotations. As CORDIC only uses bitshifting- and add/sub-operations, it is very suitable for hardware implementation of complex algorithms. The disadvantage of iterative algorithms is that they require more time, but this can be avoided by a pipelined implementation. Because the Givens rotation is based on trigonometric functions, the CORDIC is preferred for the Givens rotation in the QRD here. The principle implementation of one real valued CORDIC iteration is shown in Fig. 2. In this example the givens rotations are applied to the rows i and $(i-1)$ of the matrix $\mathbf{E}$ for QRD in (16). The results are the corresponding rows in $\mathbf{R}$ where the rotations generates $\mathbf{r}_j^{(i)} = 0$. Generally, bitshift-operations on fixed-point numbers are equivalent to a multiplication or division of two on a floating-point number depending on the shift-direction. In this case the bitshift to the right produces a low complexity and hardware efficient division by two.

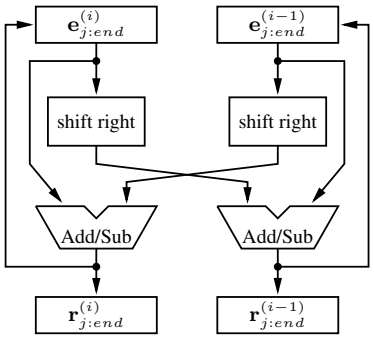

Fig. 2. Principle hardware implementation of real valued single iteration CORDIC for Givens rotation in the QRD of (16).

C. Fixed-Point Implementation

As a consequence of the iterative topology of the CORDIC algorithm, the numerical accuracy depends on the number of micro rotations. On the other hand the accuracy is reduced by a conversion from floating-point to fixed-point, which is necessary for efficient hardware. To obtain an usable quantization some simulations are necessary. The result of them is

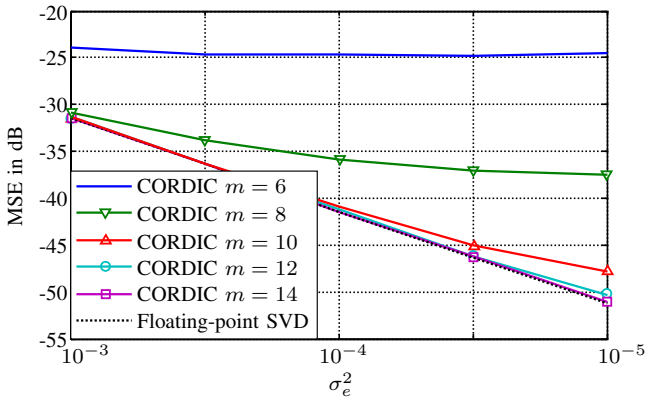

Fig. 3. Mean square error (MSE) of DL after calibration with fixed-point CORDIC (16 fractional bits). m denotes the number of micro-rotations. Reciprocity error variance σ_δ^2 is set to -20 dB, $N_B = N_M = 4$ antenna system with $N_c = 256$ subcarries and $K_c = 1$ subcarriers used for calibration.

that the floating-point SVD TLS solution can nearly be achieved by using 16 fractional bits within the CORDIC. For the results in Fig. 3 the mean square error (MSE) between the transmission channel $\overline{\mathbf{H}}$ and the calibrated UL channel $\underline{\mathbf{G}}$ depending on the estimation error variance σ_e^2 is illustrated. The reciprocity error variance is set to $\sigma_\delta^2 = -20$ dB. The effect of different numbers of micro-rotations is shown. It can be seen that the number of rotations must not be chosen to small to reach an acceptable calibration.

D. Precision/Throughput Trade-off

The precision of the calibration has a fundamental influence on the performance of the data transmission. As shown before, the number of micro-rotations has a significant impact on the accuracy of the calibrated UL channel. But more CORDIC iterations take more clock cycles in a hardware implementation, which result in a longer computation time. Otherwise, the CORDIC and the QRD can be parallelized to enhance the throughput. To get a trade-off of precision and computing time a programmable CORDIC-unit should be used, where the CORDIC is optimized for, e.g., $m = 4$ iterations. If this optimized CORDIC is used several times, multiples of 4 micro-rotations can be achieved, e.g., $m = 4$, $m = 8$ or $m = 12$. Depending on the error variance the fixed-point calibration with fewer micro-rotations is not always worse than a calibration with floating point SVD. Fig. 3 shows that with $m \geq 8$ iterations nearly the floating-point SVD TLS solution can be reached for an estimation error variance of $\sigma_e^2 = 10^{-3}$. If a short calculation time is needed, the computation time can be reduced by fewer iterations if CE and reciprocity errors allow this.

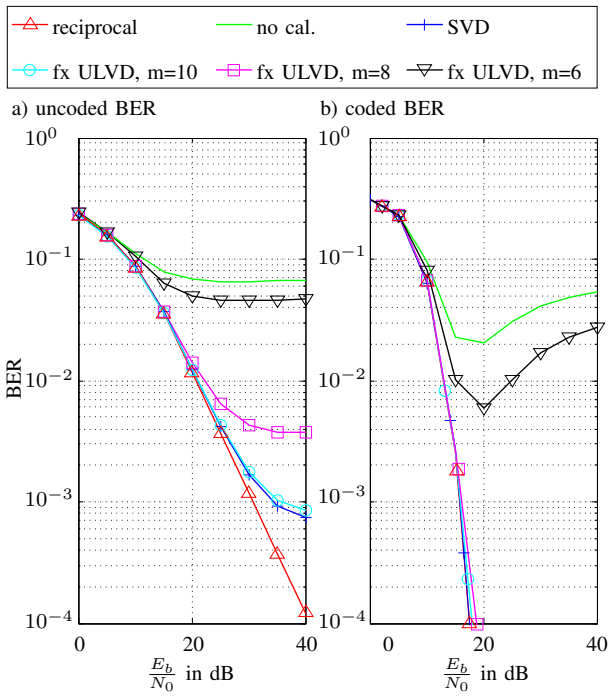

Fig. 4. BER versus E_b/N_0 for an uncalibrated and a calibrated MU-MISO system with $N_B = N_M = 4$, $N_C = 256$ subcarriers ($k_c = 3$ subcarriers used for calibration) for different numbers of micro rotations m. 16-QAM using linear MMSE pre-equalization with reciprocity error variance of $\sigma_\delta^2 = -20$ dB and a channel estimation error variance of $\sigma_e^2 = 10^{-4}$. The applied channel code in b) is a half-rate punctured Turbo Code.

V. Results

The performance evaluation presented in this paper are obtained from the described MU-MISO-OFDM system in Section II. The number of BS antennas is set to $N_B = 4$ and the number of single antenna MS is also $N_M = 4$. There are $N_c = 256$ subcarriers used for transmission and $K_c = 3$ subcarriers used for the calibration. Rayleigh fading channel model with tap length of 6 is applied. 16-QAM modulation is chosen and MMSE pre-equalization on basis of the calibrated UL channel is performed. The reciprocity error variance is set to $\sigma_\delta^2 = -20$ dB and the channel estimation error variance is set to $\sigma_e^2 = 10^{-4}$. The simulation results in Fig. 4 show the impact of micro rotations on the BER of the OFDM-system. In a) an uncoded transmission is chosen whereas in b) a half-rate punctured 3GPP Turbo Code is applied. The red lines show the BER for reciprocal UL and DL channels and perfect channel knowledge without any estimation errors. A deactivated calibration is illustrated by the green lines whereas the blue lines show the calibration with a floating-point SVD. It can be seen, that without calibration an acceptable BER cannot be achieved even if coding is used. The worse coded BER for higher E_b/N_0 is described in [2] with the dependency of the interference from a reciprocity mismatch being inversely related to the noise power. The influence of the number of micro rotations m on the uncoded BER is larger than the influence on the coded case. The difference of the calibration with a floating-point SVD and the fixed-point CORDIC based ULVD is vanishing for $m \geq 10$ in the uncoded and for $m \geq 8$ in the coded case.

VI. Conclusion

In this paper the idea of relative calibration is analysed to achieve an efficient calculation in hardware like FPGAs or VLSI circuits. It is described how the relative calibration is used to improve the MMSE precoding in MU-MISO-OFDM systems. By using the presented ULVD the complex SVD can be avoided to obtain the TLS solution, which is needed for the calibration. With the illustrated CORDIC algorithm the ULVD can be performed by two QRDs. These QRDs can efficiently be implemented in fixed-point on hardware. The simulation results demonstrate that the CORDIC needs only 10 iterations for uncoded and 8 iterations for the coded transmission to reach nearly the same BER compared to the floating-point SVD. In future works further sources of error, like mutual coupling, will be analyzed. Also the efficient hardware implementation of a recursive TLS algorithm will be investigated.

References

[1] W. Keusgen, "Antennenkonfiguration und Kalibrierungskonzepte für die Realisierung reziproker Mehrantennensysteme," PhD thesis (in German), RWTH Aachen, Germany, Oct. 2005.

[2] M. Petermann, D. Wübben, and K.-D. Kammeyer, "Evaluation of Encoded MU-MISO-OFDM Systems in TDD Mode with Non-ideal Channel Reciprocity," in *8th International ITG Conference on Source and Channel Coding (SCC)*, Siegen, Germany, Jan. 2010.

[3] M. Guillaud, "Transmission and Channel Modeling Techniques for Multiple-Antenna Communication Systems," PhD thesis, Ecole Nationale Superieure des Telecommunications, Paris, France, July 2005.

[4] G. H. Golub and C. F. Van Loan, *Matrix Computations*, Johns Hopkins Univ. Press, third edition, 1996.

[5] S. Van Huffel and J. Vandewalle, *The Total Least Squares Problem: Computational Aspects and Analysis*, Society for Industrial and Applied Mathematics (SIAM), Philadelphia, PA, USA, 1991.

[6] S. Van Huffel and H. Zha, "An efficient total least squares algorithm based on a rank-revealing two-sided orthogonal decomposition," *Numerical Algorithms*, vol. 4, no. 1, pp. 101–133, 1993.

[7] M. Petermann, M. Stefer, D. Wübben, M. Schneider, and K.-D. Kammeyer, "Low-Complexity Calibration of Mutually Coupled Non-Reciprocal Multi-Antenna OFDM Transceivers," in *The 7th International Symposium on Wireless Comm. Systems (ISWCS)*, York, UK, Sept. 2010.

[8] J. E. Volder, "The CORDIC Trigonometric Computing Technique," *IRE Transactions on Electronic Computers*, vol. EC-8, no. 3, pp. 330 –334, 1959.

[9] B. Parhami, *Computer Arithmetic Algorithms and Hardware Designs*, Oxford University Press, New York, 2000.